Aerosol and Air Quality Research, 16: 1701–1712, 2016

ISSN: 1680-8584 print / 2071-1409 online
doi: 10.4209/aaqr.2016.04.0135

Emission and Species Distribution of Mercury during Thermal Treatment of Coal Fly Ash

Yi Wang[1,2,3], Lin Shi[1,2,3*], Pen-Chi Chiang[1,4], Xiao-Fang Mou[1,2,3], Hong-Ji Liang[1,2,3]**

[1] *School of Environment and Energy, South China University of Technology, Guangzhou 510006, China*
[2] *The Key Lab of Pollution Control and Ecosystem Restoration in Industry Clusters, Ministry of Education, South China University of Technology, Guangzhou 510006, China*
[3] *Guangdong Provincial Key Laboratory of Atmospheric Environment and Pollution Control, Guangzhou 510006, China*
[4] *Graduate Institute of Environmental Engineering, National Taiwan University, Taipei 10673, Taiwan*

ABSTRACT

The thermal treatment of coal fly ash (FA) utilized by industries will inevitably lead to the emission of mercury, potentially causing atmospheric pollution. The present study is aimed at understanding the emission amount and species distribution of mercury during FA thermal treatment, and attempts were made to further provide basic data of mercury emission for environmental utilization of the FA by industries as raw materials. The physio-chemical properties of FA were analyzed and FA samples were heated at 200–1200°C in a tubular furnace in an oxidizing atmosphere. Thermogravimetric analysis (TGA) was carried out to determine the content of residual carbon in FA. The mercury species distribution was determined using United States EPA method 3200. The results indicated that semi-mobile mercury was the main mercury species in FA. Owing to the adsorption of residual carbon on Hg^0, more residual carbon which lead to higher proportion of semi-mobile obtained in coarser size grades. 20% of total mercury emitted at 206°C, followed by a rapid growth of the emission rate of mercury at above 206°C, and the emission of total mercury achieved to be 50% and 90% corresponding to 291°C and 515°C, respectively. A distinct transformation from semi-mobile mercury to extractable mercury occurred at 200°C due to catalytic oxidation of Hg^0 and enhance the mobility and potential toxicity of mercury. Both extractable and semi-mobile mercury decreased sharply at 300–400°C. Finally, the non-mobile mercury was emitted with combustion of residual carbon in FA at 600–800°C. It was thus concluded that measures would be taken to control emission of mercury for environmentally friendly utilization of coal FA by industries when the FA was heated higher than 300°C.

Keywords: Coal fly ash; Mercury; Species distribution; Emission; Thermal treatment.

INTRODUCTION

Mercury is one of the most environmentally mobile hazardous heavy metal elements, of which compounds often exhibit biological toxicity, persistence and bioaccumulation (Clarke and Sloss, 1992; Yudovich and Ketris, 2005; Jen *et al.*, 2014). Long-term exposure of high concentration of inorganic mercury poses adverse effects on the gastrointestinal tract, nervous system and kidneys of human beings (Goyer *et al.*, 2000). In addition, mercury can also be transformed to methylmercury or ethylmercury by microbial activity which tend to be accumulated in fish resulting in harm to the fish and its predators (Wheatley and Wheatley, 2000), and eventually enter the human body via the food chain (Pavlish, 2009).

Coal fly ash (FA), one type of coal combustion by-products (CCBs), with finer particles in size (i.e., 0.01–100 μm) is considered as a hazardous material (Ram and Masto, 2010). In China, the installed capacity of coal-fired power plants increased significantly since 2002 and the coal consumption reached up 2.8 billion tons in 2010 (China, 2010). China is the largest coal consumer and accounted for 50.2% of the world coal consumption in 2012 (Yao *et al.*, 2015) and coal generates about 70% of the primary energy in China (Hu *et al.*, 2015; Qin *et al.*, 2015). Annual generation of FA still increases and is anticipated to reach 580 million tons by 2015 (Yao *et al.*, 2014). It is noted that the coal FA has been successfully utilized in various applications, such as an adsorbent for CO_2 capture (Pan *et al.*, 2012) and/or a supplementary cementitious material (Pan *et al.*, 2015). However, the growing awareness of the environmental

* Corresponding author.
Tel.: +86 20 33757292; Fax: +86 20 85511266
E-mail address: celshi@scut.edu.cn
** Corresponding author.
Tel.: +886 2 23622510; Fax: +886 2 23661642
E-mail address: pcchiang@ntu.edu.tw

concerns requests a better understanding of the physico-chemical properties of FA. Therefore, there would be an urgent need for addressing this issue.

In China, the average concentration of mercury in raw coal is about 0.22 mg kg^{-1} (Wang *et al.*, 2000), which is higher than the Clarke value of mercury in the crust (0.08 mg kg^{-1}) (Wang and Wei, 1995) and global average concentration of mercury in raw coal (0.12 mg kg^{-1}) (Wang *et al.*, 2002). The combustion condition of coal, residual carbon content, coal type, presence of magnetite, chlorine concentration, and composition of the FA, are the main factors affecting the emission concentration of mercury in flue gas (Mardon and Hower, 2004; Maroto-Valer *et al.*, 2005; Chiu *et al.*, 2015). In general, the mercury content in FA is approximately 1–4 times (Yao *et al.*, 2004) higher than that in raw coal, but in some cases are lower(Wang *et al.*, 1999). In China, the emission standard for mercury from thermal power plants is 0.03 mg m^{-3} (China, 2011).

In China, the utilization ratio of FA has remained at approximately 67% in recent years, and is expected to reach 70% by 2015 (Yao *et al.*, 2015). At present, FA is widely used in construction materials, agriculture, absorbents, smelting industries, and geotechnical engineering (Kamon *et al.*, 2000; Cheng *et al.*, 2004). In these industries, heat treatment such as drying, roasting, and calcining is required before the using of FA or its mixtures. As suggested by the literature (Xu *et al.*, 2005; Cultrone and Sebastián, 2009), the preparation of the FA brick required to heated at 800–1000°C, the FA molecular sieve needed to be heated to 850°C with drying at 450–550°C, and the recovery alumina of FA require a calcining temperature in the range of 1300–1400°C. Owing to volatility and high content of the mercury in FA, it is inevitably released into the atmosphere during thermal treatment.

The residual carbon plays an important role in adsorption of mercury in FA (Li and Hwang, 1997; Serre and Silcox, 2000; Senior and Johnson, 2005; Wang and Wu, 2006) As reported, there is a positive correlation between mercury concentration and residual carbon content in FA (Hower *et al.*, 2005). FA can also be employed as a mercury adsorbent for removing gaseous mercury from flue gas (Hassett and Eylands, 1999; Serre and Silcox, 2000; Hutson, 2008). Recently, several studies have shown that Hg^0 and Hg^{2+} are the dominate chemical form of mercury in FA(Galbreath and Zygarlicke, 2000; Lopez-Anton *et al.*, 2011). The present form of Hg^{2+} was found to be $HgCl_2$ and HgO primarily, which could be adsorbed on the residual carbon surface in FA (Galbreath and Zygarlicke, 2000; Lopez-Anton *et al.*, 2011).

Based on the literature, previous studies which focused on the mercury mobility of flue gas desulphurization by-products (FGDBs) during the thermal treatment (Heebink and Hassett, 2005; Kairies *et al.*, 2006), has shown that Hg^{2+} is reduced to Hg^0 and emitted into the atmosphere at a temperature range of 150–180°C in FGDBs (Heebink and Hassett, 2005). The emission and species distribution of mercury in FA are different from FGDBs in the heat treatment process. In addition, there is a large amount of residual carbon existing in FA. However, little is known about the mercury emissions combining with transformation of mercury species during the FA thermal treatment.

The present study attempts to evaluate the emission amount of mercury and discuss species distribution of mercury in FA during the thermal treatment, and provide fundamental hazardous data of mercury emission for utilization industries of FA as raw materials. Thus, the aims of this study are to (1) analyze physico-chemical properties of FA with different particle size grades, especially to determine the residual carbon content in FA with a thermogravimetric analysis (TGA); (2) determine the total concentration and species distribution of mercury in raw/sorted FA; and (3) evaluate the emission amount and species distribution of mercury in raw/sorted FA in a thermal treatment process.

MATERIALS AND METHODS

Sample Collection and Size Segregation

The Zhujiang Co-combustion Power Plant (4 × 300 MW), equipped with a cycle power generation unit and high-efficiency electrostatic precipitators, is located in the Nansha Economic Development Zone (Guangzhou, P R China). Approximately 50 kg of FA sample was collected from the electrostatic precipitator outlets. The raw FA samples (0.1–180 μm in size) were screened into four particle size grades as sorted FA samples: > 150 μm, 75–150 μm, 54–75 μm, and < 54 μm with 100, 200, and 300 mesh sieves. The raw/sorted FA samples were heated in a tubular furnace at rate of 10 °C min^{-1} to the different final temperatures ranged from 200 to1200°C at a 2 L min^{-1} flow rate with air and held for 30 min, after which the sample was allowed to cool down to room temperature in the air.

Analysis of Physico-Chemical Characteristics of the Raw/Sorted FA

The chemical compositions of the raw/sorted FA samples were determined by X-Ray fluorescence (XRF, Axios, PANalytical Company, Netherlands). The X-Ray diffraction (XRD, D/Max-IIIA, Rigaku, Japan) was used to determine the mineral species of FA. The (Brunauer, Emmett and Teller) BET surface area of the FA samples was determined using a Micromeritics ASAP2020M apparatus. A scanning electron microscope (SEM, S-3700N, Hitachi, Japan) was used to determine the superficial morphology of the samples. A size distribution analyzer (LA-920, Horiba, Japan) was used to measure the particle sizes of FA.

The TGA was carried out using a TGA/STDA851e thermal analyzer from 50°C to 1000°C with a heating rate of 10°C min^{-1} under an air atmosphere. The residual carbon content in raw/sorted FA samples was calculated with ΔTG value, which was the weight differences from 500°C to 800°C in TGA curve. In addition, the differential scanning calorimetry (DSC) of raw FA was determined using NETZSCH STA449C thermogravimetric analyzer (50–950°C; 10 °C min^{-1}; air atmosphere). It is noted that, in the case of interference, a modified presentation on TG-DTG curves should be introduced to accurately and precisely determine the weight loss due to thermal decomposition and/or oxidation combustion (Pan *et al.*, 2016).

Sequential Extraction Experiments of Mercury Species

The raw/sorted FA sample and the FA samples with thermal treatment at different temperature were used for sequential extraction experiments, respectively. The sequential extraction procedure of United States Environmental Protection Agency (USEPA) Method 3200 was used to extract mercury species in FA samples, as shown in Fig. 1. This method provides information on both total mercury and various mercury species. According to Fig. 1, the mercury in FA samples was divided into three species, including extractable (mobile) mercury, semi-mobile mercury, and non-mobile mercury. The majority of potential mercury toxicity to the environment often derived from the extractable and semi-mobile fractions. But the non-mobile mercury fraction, such as mercury sulfide, was chemically stable in the environment.

Determination of Mercury Concentration in FA

Samples extracted by sequential extraction experiments were diluted by 5% W/V $K_2Cr_2O_7$ to 100 mL. Samples were stored at less than 4°C and analyzed completely within 5 days (Jian and McLeod, 1992). The mercury concentration was determined by an atomic fluorescence spectrometer (AFS-9130, Beijing Titan Instruments) and calculated according to Eq. (1).

$$\rho = \frac{C \times \frac{V}{A}}{M} \quad (1)$$

where ρ represents the mercury concentration (ppm); C represents the mercury concentration in the digestion liquid ($\mu g\ L^{-1}$); and M represents the quantity of the samples digested (g). The V and A are assumed to be 100 mL and 1000 mL L^{-1}, respectively.

RESULTS AND DISCUSSION

Characterization of Raw and Sorted FA

Physico-Chemical Properties

The raw FA mainly consisted of SiO_2 (34.0%) and Al_2O_3 (51.1%). The minor compositions were Fe_2O_3 and CaO of which the contents were 4.6% and 6.2%, with trace compositions of K_2O (1.2%), MgO (1.1%), TiO_2 (1.0%) and Na_2O (0.7%). According to the XRD results, the main mineral species in FA were quartz (SiO_2) and mullite ($Al_{2.8}Si_{1.2}O_{9.6}$). Rapid cooling in high temperature easily generates amorphous-phase aluminosilicate in coal combustion fly ash (Li *et al.*, 2011), and thus, the aluminosilicate glass, quartz and mullite become the major phases in FA. No significant change in mineral species with the different particle size fractions was found similar to the previous study (He *et al.*, 2015).

The raw FA was gray in color and had a cement-like appearance and the particle size ranged from 0.52 to 74.51 μm (average = 26.85 μm). Table 1 presents the specific surface area of the raw/sorted FA samples, which indicated that the BET surface area of the raw FA was found to be 3.35 $m^2\ g^{-1}$. For the sorted FA, the BET surface areas increased with the increase of FA particle size (e.g., 1.61, 2.58, 2.91, and 4.36 $m^2\ g^{-1}$ for < 54, 54–75, 75–150, and > 150 μm size grades, respectively). In general, the surface

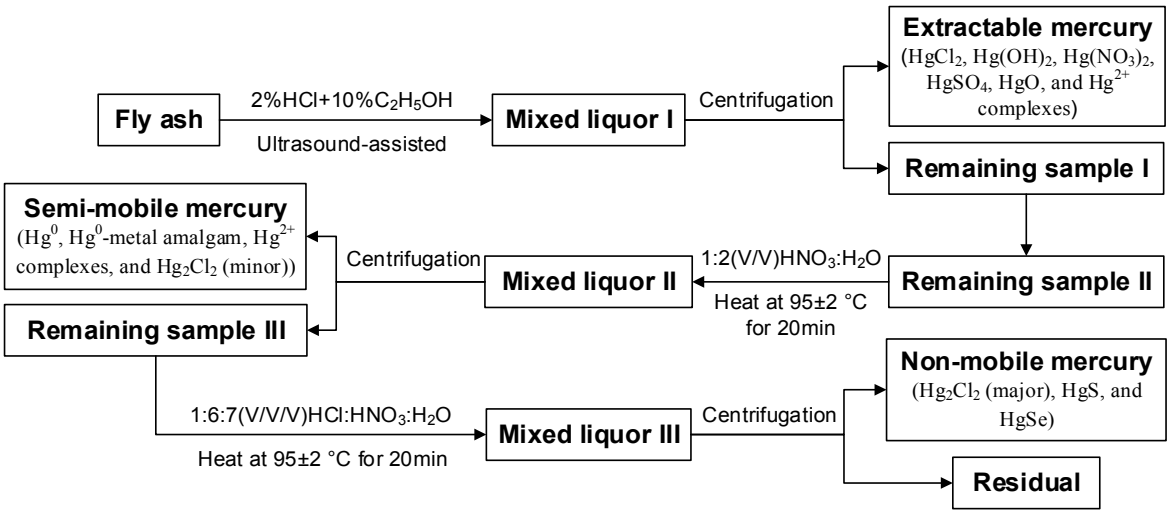

Fig. 1. Sequential extraction procedure and mercury fractions (extractable, semi-mobile and non-mobile) corresponding with individual species.

Table 1. BET surface area, LOI and total concentration of mercury in raw and sorted FA samples

Particle size grades	Units	Sorted FA				Raw FA
		> 150 μm	75–150 μm	54–75 μm	< 54 μm	
BET surface area	$m^2\ g^{-1}$	4.36 ± 0.19	2.91 ± 0.09	2.58 ± 0.33	1.61 ± 0.15	3.35 ± 0.11
LOI	%	10.21 ± 0.33	6.24 ± 0.14	6.27 ± 0.05	1.93 ± 0.14	3.61 ± 0.22
Total Hg concentration	ppm	292.4 ± 4.8	284.1 ± 5.1	332.6 ± 3.6	306.9 ± 4.1	308.9 ± 5.9

area increases with a decrease in particle size, but for the coal fly ash, the surface area mainly depends on the carbon content (Schure *et al.*, 1985). The loss of ignition (LOI) of FA with different particle sizes exhibits a similar trend as the BET surface area, which could be ascribed to the evidence that the coarser particles of coal are less likely to burn completely when compared to finer particles.

Residual Carbon Content and Surface Morphology

The residual carbon content in FA was determined by using the traditional standard method with LOI. In general, the carbon content was larger than the actual residual carbon content because the measurement of LOI included volatilization of other compounds in FA, such as $CaSO_4 \cdot 2H_2O$, $Ca(OH)_2$ and $CaSO_3 \cdot 0.5H_2O$ (Finkelman, 1995), which contained bound water or constitutional water. The bound water or constitutional water in calcium compounds can volatilize completely below 500°C (Jin *et al.*, 2005). Furthermore, a method (Ba *et al.*, 2012) of calculation by weight difference (ΔTG) before and after residual carbon combustion (500–800°C) in the TGA curve was employed to obtain a more precise residual carbon content in FA which compared with the LOI. Fig. 2 shows the relevant TG-DSC results, indicating that there is no endothermic decomposition of $CaCO_3$ in FA to affect the determination of residual carbon content obtained from the ΔTG value because of the exothermic peak at 500–800°C in DSC curve.

The weight of FA samples decreased sharply at the temperature ranging from 600 to 800°C due to the combustion of residual carbon in FA. The residual carbon content was found to be 2.8% in raw FA. For the sorted FA, a higher residual carbon content was observed than that of the raw FA with 8.9% and 5.0% in the > 150 μm and 150–75 μm size grades, respectively. The residual carbon contents of sorted FA in the 75–54 μm and < 54 μm size grades were 2.7% and 1.4%, respectively, indicating that the residual carbon content decreased with the decrease of FA particle size, which were similar to the results of previous studies (Guedes *et al.*, 2008; He *et al.*, 2015). The result represents actual residual carbon content in raw/sorted FA, which was in good agreement with the LOI results. In addition, more residual carbon existed in coarser size grades, thereby contributing to a higher BET surface area than that of FA in the fine particle size.

According to the superficial morphology determined by the SEM [Figs. 3(a)–3(d)], the FA particle can be generally divided into three categories: irregular porous particle, irregular fused structural particle, and spherical smooth particle. The FA was found to be fine powder particles and predominantly spherical in shape, either solid or hollow (Fig. 3), which were similar to the results of previous studies (Ahmaruzzaman, 2010; Van der Merwe *et al.*, 2014). The FA in > 150 μm size grade exhibited irregular spherical shape with rough edges [Fig. 3(a)]. Thus, the irregular particles combined with potential residual carbon with dark-colored porous structures were the main morphology in > 150 μm size grade. It was because that the residual carbon particles from pulverized coal combustion are irregular in shapes (He *et al.*, 2015). Similar observations were also found in previous studies (Ahmaruzzaman, 2010; Ram and Masto, 2010) that the carbonaceous material in the FA is composed of angular particles. For the FA in 75–150 and 54–75 μm size grades, as shown in Figs. 3(b) and Fig. 3(c), respectively, the fused structural particles were observed, where the particles remain predominantly irregular. The portion existence of spherical smooth glass particles was found to be <54 μm size grade, as shown in Fig. 3(d).

Figs. 3(e)–3(h) show the SEM images of the sorted FA with different size grades after heating at 800°C. Significant change in morphology of coarser size grades with more residual carbon was observed. For the > 150 μm size grade, some of the irregular particles with potential residual carbon with dark-colored porous structures nearly disappeared [Fig. 3(e)], compared to the FA without thermal treatment [Fig. 3(a)]. The edges of irregular particles became sleek, where the fused structures on the surface of particles and a

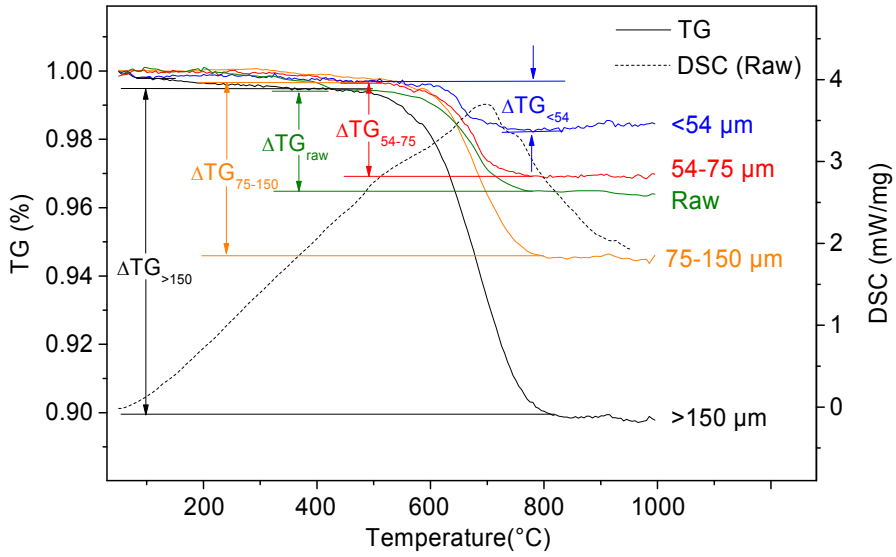

Fig. 2. TG-DSC curve and ΔTG of the raw and sorted FA samples.

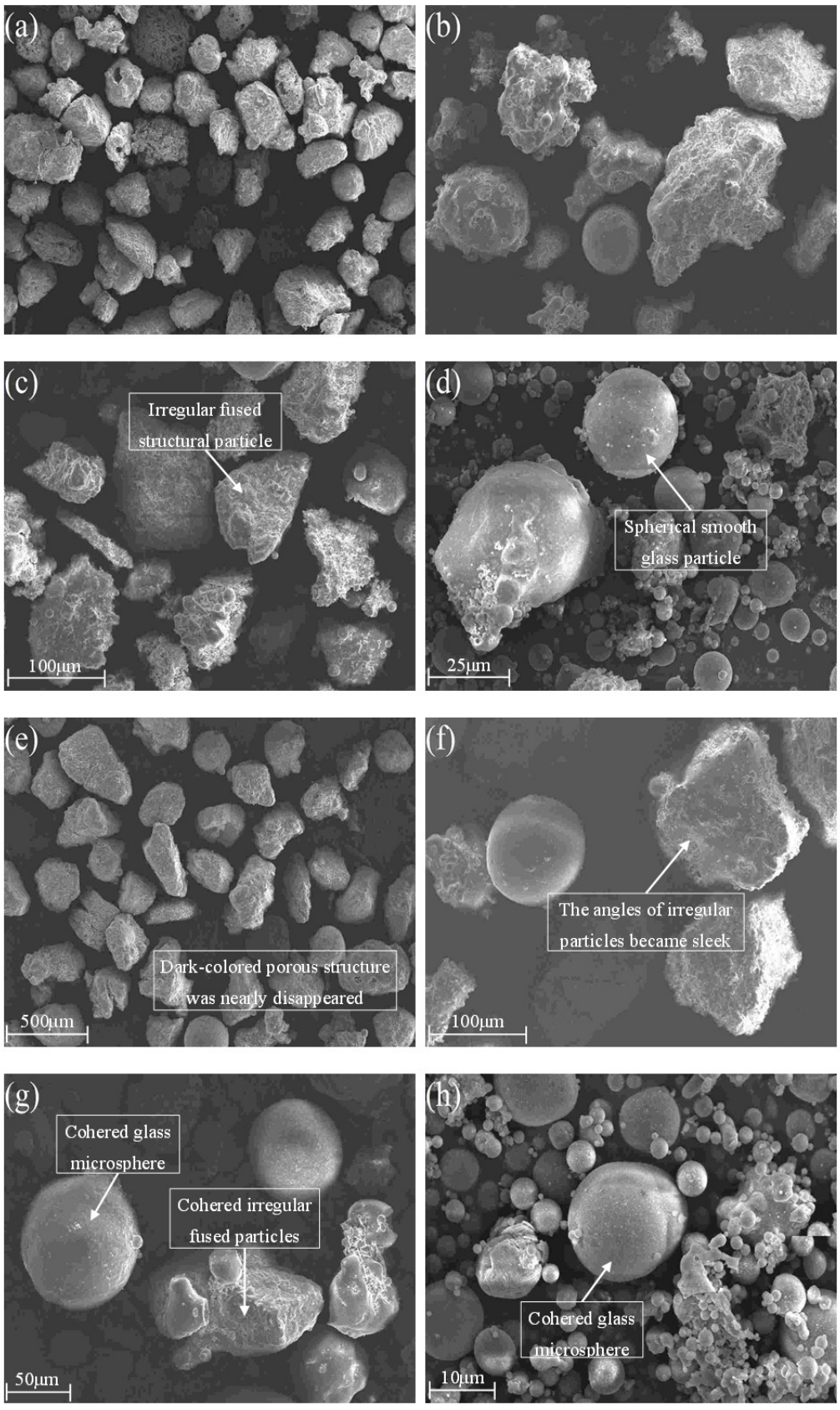

Fig. 3. Superficial morphology of the sorted FA samples without thermal treatment (a–d) and heated at 800°C (e–h). (a) > 150 μm size grade (× 50); (b) 75–150 μm size grade (x 200); (c) 54–75 μm size grade (× 300); (d) < 54 μm size grade (× 1000). (e) > 150 μm size grade (× 50); (f) 75–150 μm size grade (× 300); (g) 54–75 μm size grade (× 400); (h) < 54 μm size grade (× 2000).

small amount of cohered glass microspheres were observed in the 75–150 and 54–75 μm size grades [Figs. 3(f) and 3(g)]. For the FA with < 54 μm size grade, no significant change was found between spherical particles with least residual carbon and FA which was shown in Fig. 3(h). A binding phenomenon showed that most coherent glass spherical particles with different sizes compared to the other sorted FA was also shown in Fig. 3(h). Therefore, the SEM results suggested that the residual carbon content decreased with decreasing FA particle size.

Total Concentration and Species Distribution of Mercury in FA

Table 1 presents the total mercury concentrations of the raw/sorted FA. The concentration of total mercury in raw FA was 308.92 ng g^{-1}, and increased from 292.37 and 284.09 ng g^{-1} in the >150 and 75–150 μm size grades to 332.63 and 306.92 ng g^{-1} in the 54–75 and < 54 μm size grades, respectively. The mercury species of the FA samples, followed by EPA Method 3200 (U.S., 2005), including the extractable mercury, the semi-mobile mercury, and the non-mobile mercury, were determined and shown in Fig. 4. Since the extractable and semi-mobile mercury in FA were mainly derived from coal-fired flue gas, most of the mercury in raw coal was gasified and emitted in the process of coal combustion, and then the gaseous mercury was catalytically oxidized and condensed to the FA particle surface. The extractable mercury concentration in raw FA was 45.6 ng g^{-1}, exhibiting slight change in the range of 43.4–48.7 ng g^{-1} with different FA particle size grades. The semi-mobile mercury concentrations of the FA in > 150, 75–150, 54–75, and < 54 μm size grades were 228.9, 218.3, 236.2, and 205.6 ng g^{-1}, respectively, accounted for 78.3%, 76.8%, 71.0%, and 67.0% of total mercury, respectively. In general, the semi-mobile mercury concentration in raw FA was 216.0 ng g^{-1} (69.9% of the total mercury). It was noted that the semi-mobile mercury was mainly derived from Hg^0 absorbed in FA residual carbon due to its stronger adsorption capacity for Hg^0 (Ba *et al.*, 2012). As a result, the coarser size grades (> 150 and 75–150 μm size grades) having the higher residual carbon content absorbed more Hg^0 (semi-mobile mercury) than the finer size grades (54–75 and < 54 μm size grades) containing less residual carbon.

The non-mobile mercury concentration in raw FA was 47.2 ng g^{-1} (15.3% of the total mercury). For the sorted FA, the non-mobile mercury concentration was approximately 18 ng g^{-1} (about 6% of total mercury) in the > 150 and 75–150 μm size grades, and increased to 53.0 and 55.4 ng g^{-1} (16.0% and 18.0% of the total mercury) in the 54–75 and < 54 μm size grades, respectively. Non-mobile mercury in FA may be derived from minerals and other non-combustible ash in raw coal. This mercury fraction cannot be gasified and emitted in the process of coal combustion (Bhardwaj *et al.*, 2009), which indicates that the extractable and semi-mobile mercury were mainly enriched in the coarser size grades and the non-mobile mercury was mainly enriched in the finer size grades (Fig. 4). A higher total mercury concentration was found in the finer size grades (Table 1) and attributed to the more non-mobile mercury that existed in the finer size grade.

Emission and Species Distribution of Mercury in FA during the Thermal Treatment

Total Emission of Mercury in Raw FA

The relationship between total emission of mercury and temperature is presented in Fig. 5, and the result indicates that the total mercury concentrations decreased with an increase in temperature from 200°C to 1200°C. The variation in mercury emissions could be depicted by four stages: (1) the total mercury had a slight decrease of 16.3% around 200°C; (2) total mercury reduced dramatically with a decrement of 55.1% to 78.1% at 300 and 400°C, respectively; (3) the total mercury concentration further decreased by 85.1% and 96.5% at 600°C and 800°C, respectively; and (4) the mercury was not observed between 1000°C and 1200°C.

Considering the transformation of mercury species in

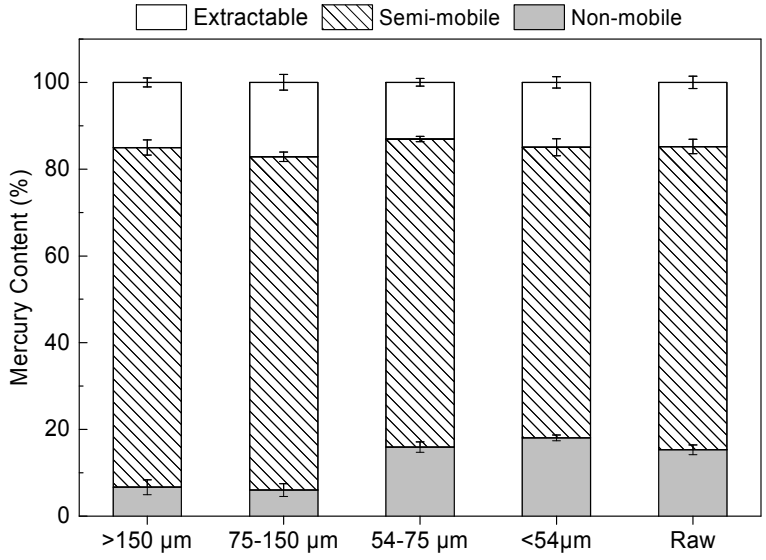

Fig. 4. Mercury species and concentrations with the error bar (standard deviation) in raw/sorted FA samples.

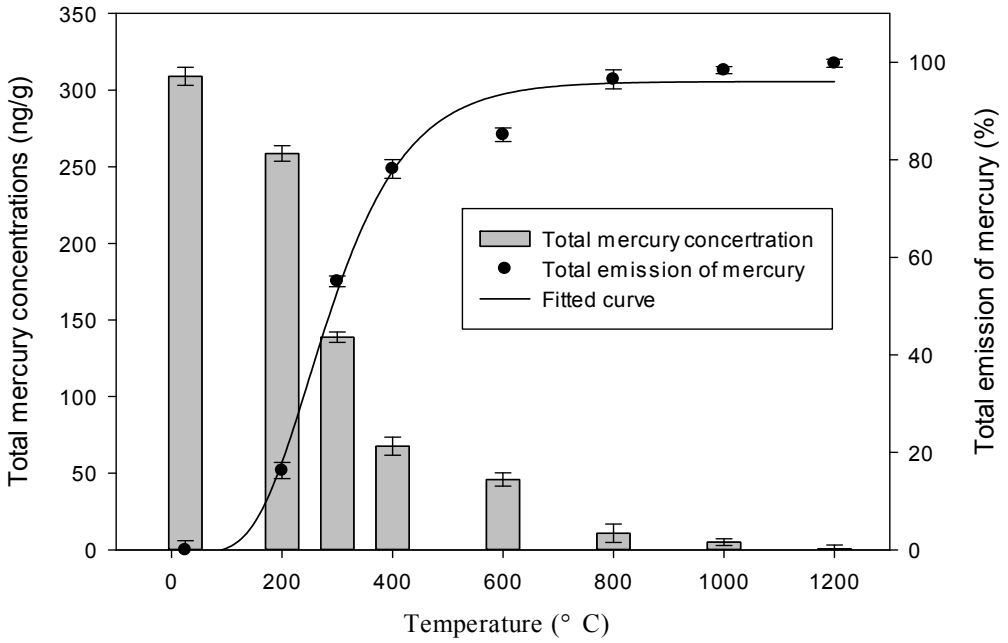

Fig. 5. Total mercury concentrations and total emission of mercury with the error bar (standard deviation) in raw FA sample during thermal treatment.

FA, the lower emission rate of mercury at low temperature (< 200°C) was obtained, as shown in Fig. 5. Afterwards, most of mercury would emit with higher emission rate at middle temperature (200–600°C), and the emission rate appears to be slow at higher temperature (600–1200°C), which indicates that the process of mercury emission during thermal treatment was fitted by sigmoidal curves (Spiess *et al.*, 2008), as shown in Eq. (2) and Eq. (3). The relationship between total emission of mercury and temperatures can be expressed by Eq. (2), in which the parameters a, b, c, d and e represent as the slope, ground asymptote (initial total emission of mercury), maximum asymptote (maximum total emission of mercury), the inflection point and additional asymmetry, respectively (Spiess *et al.*, 2008). It was assumed that the initial total emission of mercury was zero, as shown in Eq. (3).

$$y = b + \frac{c-b}{\left(1+e^{(a(x-d))}\right)^{e}} \quad (2)$$

$$y = \frac{c}{\left(1+e^{(a(x-d))}\right)^{e}} \quad (3)$$

The distribution of mercury emission was achieved by the fitted equation and constants shown in Table 2. The total emission rate of mercury from the FA samples increased sharply in a range of 20–90%. The corresponding emitting temperatures can be calculated by equation 2. For the raw FA, 20% and 50% of total mercury emitted at 206°C and 291°C, respectively. The total emission rate reached 90% when the temperature rose to 515°C. Similar observations were also found in previous study (Fernández-Miranda *et al.*, 2015), which indicates that the mercury in different FA is released at the temperature ranged from about 150°C to 500°C due to the emission of Hg^{2+} complexes in FA, such as Hg-OM, $HgCl_2$ and HgS, of which desorption temperatures are between 138°C and 500°C (Biester and Scholz, 1996; Zhang, 2012; Fernández-Miranda *et al.*, 2015).

Species Distribution of Mercury in FA

Fig. 6 illustrates the variation of species distribution of mercury in FA during the thermal treatment. At the temperature of 200°C, the semi-mobile mercury in raw/sorted FA decreased significantly (64.1–70.2%); however, the extractable mercury increased greatly by 2.0–2.7 folds compared with the FA sample without thermal treatment. Part of the semi-mobile mercury in raw/sorted FA has been transformed into the extractable mercury at 200°C. The transformation amounts of semi-mobile mercury in the > 150, 75–150, 54–75, and < 54 μm size grades and raw FA were 118.4 ± 3.5, 115.5 ± 4.3, 110.5 ± 2.1, 91.8 ± 0.9, and 101.1 ± 2.9 ng g^{-1}, respectively, corresponding to the conversion ratio of 51.7%, 52.9%, 46.8%, 44.6%, and 46.8%, respectively.

Table 2. Constants and correlation coefficients of the fitted curve for mercury emission from the raw FA samples during thermal treatment.

Parameters	a	c	d	e	r^2
Value	–0.01027	0.9604	–497.07	2121.38	0.991

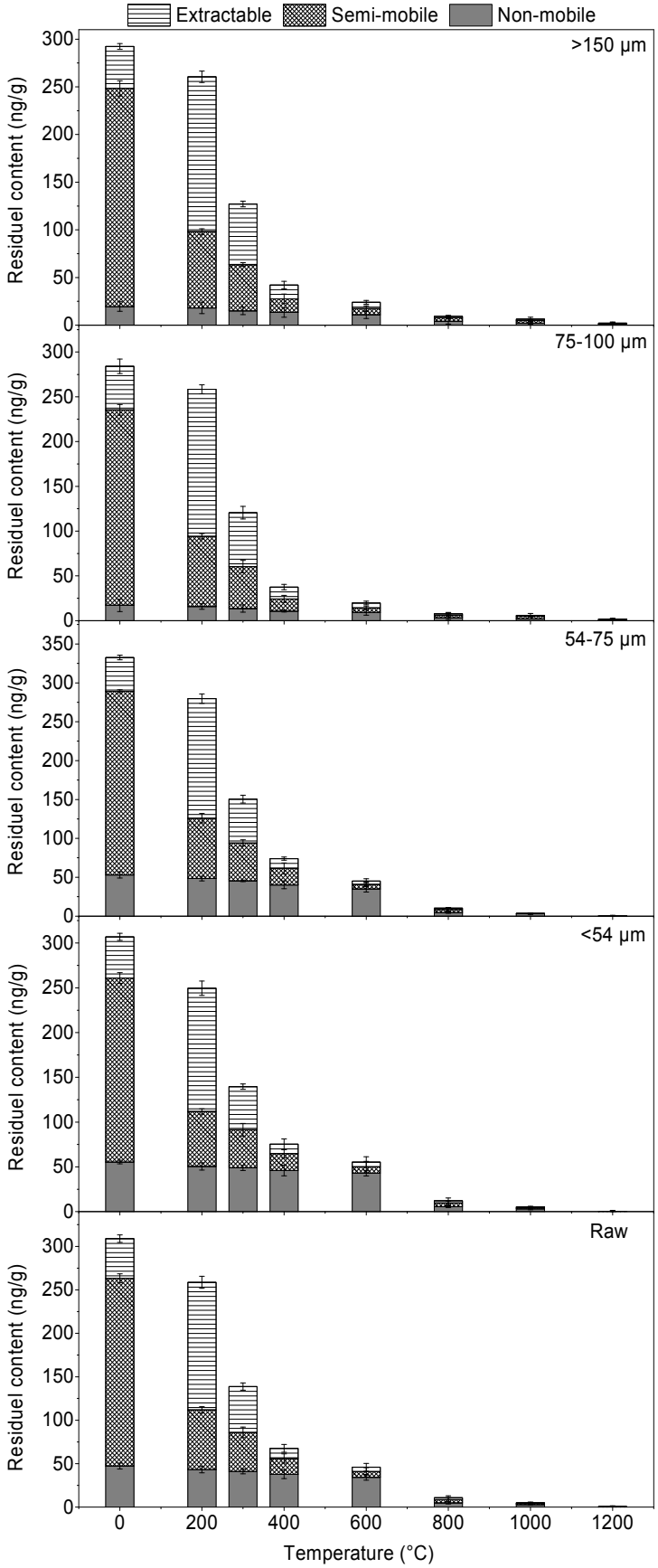

Fig. 6. Species distribution of mercury with the error bar (standard deviation) in raw/sorted FA samples during thermal treatment.

The above mercury transformation process could be explained by the Mars-Maessen model (Granite *et al.*, 2000), as shown in Eqs. (4–7). Some of the Hg^0 as a major species of semi-mobile mercury was oxidized into Hg^{2+} at 200°C in an oxidizing atmosphere causing the increasing dramatically of extractable mercury. In an oxidizing atmosphere, Hg^0 is easily oxidized by direct oxidation with gas-phase oxygen to HgO (Eq. (4)) and catalytic oxidation with a catalyst, such as inorganic constituents (López-Antón *et al.*, 2007; Bartoňová *et al.*, 2012) and residual carbon (Sakulpitakphon *et al.*, 2000; Dunham *et al.*, 2003), and then leading to the formation of Hg^{2+} complexes (Granite *et al.*, 2000; Pena *et al.*, 2001) and HgO (extractable mercury) (Galbreath and Zygarlicke, 2000).

$$2Hg + O_2 \rightarrow 2HgO_{(FA)} \quad (4)$$

$$Hg + M_xO_y \rightarrow HgO + M_xO_{y-1} \quad (5)$$

$$Hg + M_xO_{y-1} + 1/2\ O_2 \rightarrow HgO + M_xO_y \quad (6)$$

$$HgO + M_xO_y \rightarrow HgM_xO_{y+1} \quad (7)$$

Moreover, the reaction mechanism for catalytic oxidation of Hg^0 can be illustrated by Eqs. (5–7) (M_xO_y - metallic oxides). At temperatures between 300 and 400°C, both extractable and semi-mobile mercury which is mainly exists as Hg^{2+} (e.g., HgO, HgS and $HgCl_2$) (Biester and Scholz, 1996; Biester and Zimmer, 1998; Tandy *et al.*, 2004) in heated FA was sharply reduced by 58.9–64.0% and 87.9–90.0%, respectively, and had a further decrease of 95.1–96.4% at 600°C. At a temperature range of 800–1200°C, both extractable and semi-mobile mercury had little variation and the emission rate was 96.0–97.3% at 800°C, 97.8–98.9% at 1000°C, and 97.9–99.9% at 1200°C.

In the heating process, the non-mobile mercury concentration remained constant at temperatures ranging from 200°C to 400°C. As the heating temperature increased to 600°C, the non-mobile mercury in the coarser size grade was reduced by approximately 45%, which was higher than the finer size grade and raw materials by 20–30%. At a temperature of 800°C, the non-mobile mercury in the coarser size grade was reduced dramatically by approximately 80%, which was lower than the finer size grade and raw materials by approximately 90%. Thus, the emission of non-mobile mercury with combustion of residual carbon in FA sample occurred mainly at 600°C, and almost completely disappeared at 800°C (Fig. 2).

According to the above evidence, the mechanism of desorption process of mercury on the residual carbon in FA could be proposed, as shown in Fig. 7. In the thermal treatment process, the emission characteristic of mercury could be briefly divided into three stages: (1) transformation of semi-mobile mercury (Hg^0) into extractable mercury (Hg^{2+}) occurred at 200°C; (2) both extractable and semi-mobile mercury emitted dramatically from 300°C to 400°C; and (3) non-mobile mercury emitted from 600°C to 800°C due to combustion of residual carbon, which also decreased significantly from 600°C to 800°C, according to the TGA curve (Fig. 2).

Strategies on Controlling the Emission of Mercury in FA

Since the utilization of coal FA by industries generally requires the thermal treatment, emission of mercury in FA occurred inevitably during the thermal treatment due to the high mercury content in FA. At the heating temperature of approximate 200°C or slightly higher, only a small fraction of the total mercury is emitted without control, but the species transformation of mercury in FA enhance the mobility and potential toxicity of mercury. It suggests that FA should be pretreated by physical washing for removal of mercury before utilization (Senior *et al.*, 2000; Pavlish *et al.*, 2003), and physical separation and hydrothermal treatment for removal of residual carbon in FA (Timpe *et al.*, 2001). Furthermore, in the drying and dewatering process of coal FA, the heating temperature should be less than 150°C to reduce the mobility and potential toxicity of mercury. However, measures should be taken to control mercury emissions for environmentally concerned, when the FA was heated higher than 300°C, in the course of roasting and.

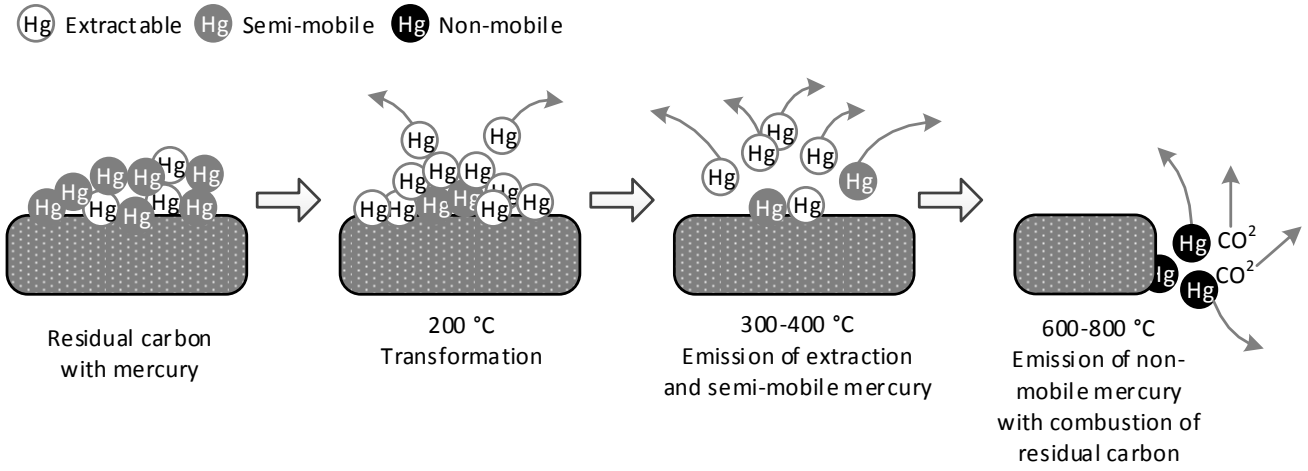

Fig. 7. Mechanism of desorption process of mercury on the residual carbon in FA.

calcining. For instance, cleaning measures such as physical cleaning with reagents (Jacobsen *et al.*, 1992), solvent extraction (Yoshiie *et al.*, 2012), froth flotation (Smit *et al.*, 1996) and heavy-media cyclone separator (Ferris *et al.*, 1992), so called green technology, are the preventive solution to eliminate the mercury content in coal prior to combustion

Significant control of mercury emissions from coal fly ash during the thermal treatment can be achieved by limiting the amount of mercury entering into the coal fly ash in the coal combustion. The air pollution control technologies for mercury removal, such as sorbent injection (Pavlish *et al.*, 2003), wet scrubbing (Pavlish *et al.*, 2003), spray dryer absorbers (Chu, 2000; Senior *et al.*, 2000), and carbon capture (Na *et al.*, 2014), also should also be applied. In addition, the relevant environmental laws, standards and regulations should be imminently established and enforced to limit the mercury emissions during the thermal treatment process, and to restrict mercury content of FA in the utilization of coal FA by industries via an integrated waste management plan (IWMP) throughout the life cycle assessment (LCA).

CONCLUSIONS

A proxy measurement for residual carbon content of FA was determined between 500°C and 800°C in TGA curves, which indicates that the residual carbon increased significantly as the FA particle size increased. The SEM images also indicated more residual carbon content was observed in a coarser FA particle size, while the glass microsphere existed in a finer FA particle size. There was no significant difference in total mercury contents in different particle size grades. Considering the different speciation of mercury in the FA, the dominant fraction in all particle size grades was the semi-mobile fraction, which accounted for at least 65% of total mercury. The content of non-mobile mercury in the coarser FA particle size grades is three times less than the finer particles.

The mercury began to emit at approximately 200°C and almost completely emitted at 1200°C in the raw FA sample. 20% of the total mercury could emit at 206°C, and the emission rate of mercury, increasing sharply at temperatures higher than 206°C, reached 50% and 90% at 291°C and 515°C, respectively. A distinct transformation from semi-mobile mercury to extractable mercury was observed in the FA at 200°C. Both extractable and semi-mobile mercury decreased dramatically from 300°C to 400°C. The non-mobile mercury decreased significantly with combustion of residual carbon from 600°C to 800°C. Therefore, measures should be taken to control emission of mercury for the environmentally friendly utilization of coal FA by industries when the FA is heated higher than 300°C.

ACKNOWLEDGEMENTS

The authors gratefully acknowledge the Natural Sciences Foundation of Guangdong Province (Project S2011020005187), and the Science and Technology Plan of Guangdong Province (Project 2013B020700006).

REFERENCES

Ahmaruzzaman, M. (2010). A review on the utilization of fly ash. *Prog. Energy Combust. Sci.* 36: 327–363.

Ba, B., Shi, L. and Mou, X.F. (2012). Mercury emissions from coal fly ash and the influence of unburned carbon during thermal treatment. *Fresenius Environ. Bull.* 21: 1885–1893.

Bartoňová, L., Čech, B., Ruppenthalová, L., Majvelderová, V., Juchelková, D. and Klika, Z. (2012). Effect of unburned carbon content in fly ash on the retention of 12 elements out of coal-combustion flue gas. *J. Environ. Sci.* 24: 1624–1629.

Bhardwaj, R., Chen, X. and Vidic, R.D. (2009). Impact of fly ash composition on mercury speciation in simulated flue gas. *J. Air Waste Manage. Assoc.* 59: 1331–1338.

Biester, H. and Scholz, C. (1996). Determination of mercury binding forms in contaminated soils: Mercury pyrolysis versus sequential extractions. *Environ. Sci. Technol.* 31: 233–239.

Biester, H. and Zimmer, H. (1998). Solubility and changes of mercury binding forms in contaminated soils after immobilization treatment. *Environ. Sci. Technol.* 32: 2755–2762.

Cheng, J., Zhou, J.H., Liu, J.Z., Cao, X.Y., Zhou, Z.J., Huang, Z.Y., Zhao, X. and Cen, K.F. (2004). Physicochemical properties of chinese pulverized coal ash in relation to sulfur retention. *Powder Technol.* 146: 169–175.

China, N.B.o.S.o. (2010). *China Statistical Yearbook*.

China, N.S.o.t.P.s.R.o. (2011). Gb13223: Emission Standard of Air Pollutants for Thermal Power Plants.

Chiu, C., Lin, H., Kuo, T., Chen, S., Chang, T., Su, K. and Hsi, H. (2015). Simultaneous control of elemental mercury/sulfur dioxide/nitrogen monoxide from coal-fired flue gases with metal oxide-impregnated activated carbon. *Aerosol Air Qual. Res.* 15: 2094–2103.

Chu, P. (2000). *An Assessment of Mercury Emission from Us Coal-Fired Power Plants*. Electric Power Research Institute.

Clarke, L.B. and Sloss, L.L. (1992). *Trace Elements-Emissions from Coal Combustion and Gasification*. IEA Coal Research.

Cultrone, G. and Sebastián, E. (2009). Fly ash addition in clayey materials to improve the quality of solid bricks. *Constr. Build. Mater.* 23: 1178–1184.

Dunham, G.E., DeWall, R.A. and Senior, C.L. (2003). Fixed-bed studies of the interactions between mercury and coal combustion fly ash. *Fuel Process. Technol.* 82: 197–213.

Fernández-Miranda, N., Rumayor, M., Lopez-Anton, M.A., Díaz-Somoano, M. and Martínez-Tarazona, M.R. (2015). Mercury retention by fly ashes from oxy-fuel processes. *Energy Fuels* 29: 2227–2233.

Ferris, D., Bencho, J. and Torak, E. (1992). Engineering Development of Advanced Physical Fine Coal Cleaning Technologies-Froth Flotation; Icf Kaiser Engineers Final Report for Doe Contract No. *DEAC22-88PC88881*.

Finkelman, R.B. (1995). Modes of Occurrence of Environmentally-Sensitive Trace Elements in Coal, In

Environmental Aspects of Trace Elements in Coal, Springer, pp. 24–50.

Galbreath, K.C. and Zygarlicke, C.J. (2000). Mercury transformations in coal combustion flue gas. *Fuel Process. Technol.* 65: 289–310.

Goyer, R.A., Aposhian, V., Arab, L., Bellinger, D., Burbacher, T., Burke, T., Jacobson, J., Knobeloch, L., Stern, A. and Ryan, L. (2000). *Toxicological Effects of Methylmercury*. Washington, DC: National Research Council: 368.

Granite, E.J., Pennline, H.W. and Hargis, R.A. (2000). Novel sorbents for mercury removal from flue gas. *Ind. Eng. Chem. Res.* 39: 1020–1029.

Guedes, A., Valentim, B., Prieto, A., Sanz, A., Flores, D. and Noronha, F. (2008). Characterization of fly ash from a power plant and surroundings by micro-Raman spectroscopy. *Int. J. Coal Geol.* 73: 359–370.

Hassett, D.J. and Eylands, K.E. (1999). Mercury capture on coal combustion fly ash. *Fuel* 78: 243–248.

He, P., Jiang, X., Wu, J., Pan, W. and Ren, J. (2015). Characterization of fly ash from coal-fired power plant and their properties of mercury retention. *Surf. Rev. Lett.* 22: 1550018.

Heebink, L.V. and Hassett, D.J. (2005). Mercury release from fgd. *Fuel* 84: 1372–1377.

Hower, J., Robl, T., Anderson, C., Thomas, G., Sakulpitakphon, T., Mardon, S. and Clark, W. (2005). Characteristics of coal combustion products (CCP's) from Kentucky power plants, with emphasis on mercury content. *Fuel* 84: 1338–1350.

Hu, X., Luo, G. and Yao, H. (2015). No reduction scale of three typical chinese coals during oxy-coal combustion. *Aerosol Air Qual. Res.* 15: 1125–1129.

Hutson, N.D. (2008). Mercury capture on fly ash and sorbents: The effects of coal properties and combustion conditions. *Water Air Soil Pollut. Focus* 8: 323–331.

Jacobsen, P., Blinn, M., Wan, E. and Nowak, M. (1992). The Role of Coal Preparation in the Precombustion Control of Hazardous Air Pollutants, In Proceedings of Coal Prep 92.

Jen, Y.H., Chen, W.H., Hung, C.H., Yuan, C.S. and Ie, I.R. (2014). Field measurement of total gaseous mercury and its correlation with meteorological parameters and criteria air pollutants at a coastal site of the Penghu Islands. *Aerosol Air Qual. Res.* 14: 364–375.

Jian, W. and McLeod, C.W. (1992). Rapid sequential determination of inorganic mercury and methylmercury in natural waters by flow injection: Cold vapour-atomic fluorescence spectrometry. *Talanta* 39: 1537–1542.

Jin, L.H., Yue, D.L. and Xu, Z.D. (2005). Morphology and physical properties of calcium zincate. *Chin. J. Inorg. Chem.* 2: 022.

Kairies, C.L., Schroeder, K.T. and Cardone, C.R. (2006). Mercury in gypsum produced from flue gas desulfurization. *Fuel* 85: 2530–2536.

Kamon, M., Katsumi, T. and Sano, Y. (2000). Msw fly ash stabilized with coal ash for geotechnical application. *J. Hazard. Mater.* 76: 265–283.

López-Antón, M., Diaz-Somoano, M. and Martínez-Tarazona, M. (2007). Retention of elemental mercury in fly ashes in different atmospheres. *Energy Fuels* 21: 99–103.

Li, H., Zhang, J., Zhao, Y., Wu, C.Y. and Zheng, C. (2011). Wettability of fly ashes from four coal-fired power plants in China. *Ind. Eng. Chem. Res.* 50: 7763–7771.

Li, Z. and Hwang, J.Y. (1997). Mercury Distribution in Fly Ash Components, In Air & Waste Management Association 90. Annual Metting.

Lopez-Anton, M.A., Perry, R., Abad-Valle, P., Díaz-Somoano, M., Martínez-Tarazona, M.R. and Maroto-Valer, M.M. (2011). Speciation of mercury in fly ashes by temperature programmed decomposition. *Fuel Process. Technol.* 92: 707–711.

Mardon, S.M. and Hower, J.C. (2004). Impact of coal properties on coal combustion by-product quality: examples from a kentucky power plant. *Int. J. Coal Geol.* 59: 153–169.

Maroto-Valer, M.M., Zhang, Y.Z., Granite, E.J., Tang, Z. and Pennline, H.W. (2005). Effect of porous structure and surface functionality on the mercury capacity of a fly ash carbon and its activated sample. *Fuel* 84: 105–108.

Na, C., Yuan, J., Xu, Y. and Hu, Z. (2014). Penetration of clean coal technology and its impact on China's power industry. *Energy Strat. Rev.* 7: 1–8.

Pan, S.Y., Chang, E.E. and Chiang, P.C. (2012). CO_2 capture by accelerated carbonation of alkaline Wastes: A review on its principles and applications. *Aerosol Air Qual. Res.* 12: 770–791.

Pan, S.Y., Chiang, A., Chang, E.E., Lin, Y.P., Kim, H. and Chiang, P.C. (2015). An innovative approach to integrated carbon mineralization and waste utilization: A review. *Aerosol Air Qual. Res.* 15: 1072–1091.

Pan, S.Y., Chang, E.E., Kim, H., Chen, Y.H. and Chiang, P.C. (2016). Validating carbonation parameters of alkaline solid wastes via integrated thermal analyses: Principles and applications. *J. Hazard. Mater.* 307: 253–262.

Pavlish, J.H., Sondreal, E.A., Mann, M.D., Olson, E.S., Galbreath, K.C., Laudal, D.L. and Benson, S.A. (2003). Status review of mercury control options for coal-fired power plants. *Fuel Process. Technol.* 82: 89–165.

Pavlish, J.H. (2009). Preface to the AQVI special issue of fuel processing technologies entitled: Air quality VI: Mercury, trace elements, SO_3, particulate matter, and greenhouse gases. *Fuel Process. Technol.* 90: 1327–1332.

Pena, J.M., Allen, N.S., Edge, M., Liauw, C.M., Santamaria, F., Noiset, O. and Valange, B. (2001). Factors affecting the adsorption of stabilisers on to carbon black (flow micro-calorimetry and FTIR studies) Part I Primary phenolic antioxidants. *J. Mater. Sci.* 36: 2885–2898.

Qin, L., Zhang, Y., Han, J. and Chen, W. (2015). Influences of waste iron residue on combustion efficiency and polycyclic aromatic hydrocarbons release during coal catalytic combustion. *Aerosol Air Qual. Res.* 15: 2720–2729.

Ram, L.C. and Masto, R.E. (2010). An appraisal of the potential use of fly ash for reclaiming coal mine spoil. *J. Environ. Manage.* 91: 603–617.

Sakulpitakphon, T., Hower, J.C., Trimble, A.S., Schram,

W.H. and Thomas, G.A. (2000). Mercury capture by fly ash: Study of the combustion of a high-mercury coal at a utility boiler. *Energy Fuels* 14: 727–733.

Schure, M., Soltys, P.A., Natusch, D.F. and Mauney, T. (1985). Surface area and porosity of coal fly ash. *Environ. Sci. Technol.* 19: 82–86.

Senior, C., Helble, J. and Sarofim, A. (2000). In Proceedings, Air Quality Control II, Mercury, Trace Elements, and Particulate Matter Conference, 2000, pp. 19–21.

Senior, C.L. and Johnson, S.A. (2005). Impact of carbon-in-ash on mercury removal across particulate control devices in coal-fired power plants. *Energy Fuels* 19: 859–863.

Serre, S.D. and Silcox, G.D. (2000). Adsorption of elemental mercury on the residual carbon in coal fly ash. *Ind. Eng. Chem. Res.* 39: 1723–1730.

Smit, F.J., Moro, N., Shields, G.L, Jha, M.C. and Feeley, TJ. (1996). Reduction of Toxic Trace Elements in Coal by Advanced Coal Cleaning. Proceedings of the 13th Annual International Pittsburgh Coal Conference, Vol. 2, Pittsburgh, PA, University of Pittsburgh, Pittsburgh, PA 1996, pp. 879–884.

Spiess, A.N., Feig, C. and Ritz, C. (2008). Highly accurate sigmoidal fitting of real-time pcr data by introducing a parameter for asymmetry. *BMC Bioinf.* 9: 221.

Tandy, S., Bossart, K., Mueller, R., Ritschel, J., Hauser, L., Schulin, R. and Nowack, B. (2004). Extraction of heavy metals from soils using biodegradable chelating agents. *Environ. Sci. Technol.* 38: 937–944.

Timpe, R., Mann, M., Pavlish, J. and Louie, P. (2001). Organic sulfur and hap removal from coal using hydrothermal treatment. *Fuel Process. Technol.* 73: 127–141.

U.S., E.P.A. (2005). Method 3200: Mercury Species Fractionation and Quantification by Microwave Assisted Extraction, Selective Solvent Extraction and/or Solid Phase Extraction.

Van der Merwe, E., Prinsloo, L.C., Mathebula, C.L., Swart, H., Coetsee, E. and Doucet, F. (2014). Surface and bulk characterization of an ultrafine south african coal fly ash with reference to polymer applications. *Appl. Surf. Sci.* 317: 73–83.

Wang, L.G. and Che, C. (2004). Elemental mercury adsorption by residual carbon separated from fly ash. *J. Uni. Sci. Technol. B.* 26: 353–356.

Wang, Q.C., Shen, W.G. and Ma, Z.W. (1999). The estimation of mercury emission from coal combustion in China. *China Environ. Sci.* 19: 318–321.

Wang, Q.C., Shen, W.G. and Ma, Z.W. (2000). Estimation of mercury emission from coal combustion in China. *Environ. Sci. Technol.* 34: 2711–2713.

Wang, Q.H., Qiu, J.R. and Wu, H. (2002). Recent advances in the study of mercury release in a coal combustion process. *J. Eng. Thermal. Energy Power* 17: 547–550.

Wang, S.B. and Wu, H.W. (2006). Environmental-benign utilisation of fly ash as low-cost adsorbents. *J. Hazard. Mater.* 136: 482–501.

Wang, Y. and Wei, F.S. (1995). *Soil Environmental Elementary Chemistry*. China Environmental Science Press.

Wheatley, B. and Wheatley, M.A. (2000). Methylmercury and the health of indigenous peoples: A risk management challenge for physical and social sciences and for public health policy. *Sci. Total Environ.* 259: 23–29.

Xu, L.L., Guo, W., Wang, T. and Yang, N.R. (2005). Study on fired bricks with replacing clay by fly ash in high volume ratio. *Constr. Build. Mater.*19: 243–247.

Yao, D.X., Zhi, X.C. and Zheng, B.S. (2004). The transformation and concentration of 5 Trace elements during coal combusion. *Environ. Chem.* 23: 31–37.

Yao, Z.T., Xia, M.S., Sarker, P.K. and Chen, T. (2014). A review of the alumina recovery from coal fly ash, with a focus in china. *Fuel* 120: 74–85.

Yao, Z.T., Ji, X.S., Sarker, P.K., Tang, J.H., Ge, L.Q., Xia, M.S. and Xi, Y.Q. (2015). A comprehensive review on the applications of coal fly ash. *Earth Sci. Rev.* 141: 105–121.

Yoshiie, R., Watanabe, H., Uemiya, S., Furuya, A., Okuyama, N. and Komatsu, N. (2012). Mercury separation from fuel constituents in an ash-free coal manufacturing process. *Fuel* 102: 26–31.

Yudovich, Y.E. and Ketris, M.P. (2005). Mercury in coal: a review Part 2. Coal use and environmental problems. *Int. J. Coal Geol.* 62: 135–165.

Zhang, B. (2012). Mercury Release Characteristics During Thermal Treatment of Fly Ash from Mws Incinerator, Huazhong University of Science & Technology, pp. 38–39.

Received for review, April 2, 2016
Revised, May 31, 2016
Accepted, June 2, 2016